JOURNAL OF VIROLOGY, May 2005, p. 5304–5314 Vol. 79, No. 9
0022-538X/05/$08.00+0 doi:10.1128/JVI.79.9.5304–5314.2005

Complete Genome Sequence and In Planta Subcellular Localization of Maize Fine Streak Virus Proteins

Chi-Wei Tsai,[1] Margaret G. Redinbaugh,[2,3] Kristen J. Willie,[3] Sharon Reed,[1] Michael Goodin,[4] and Saskia A. Hogenhout[1]*

Department of Entomology[1] and Department of Plant Pathology,[2] Ohio Agricultural Research and Development Center, The Ohio State University, and U.S. Department of Agriculture,[3] Wooster, Ohio, and Department of Plant Pathology, University of Kentucky, Lexington, Kentucky[4]

Received 3 September 2004/Accepted 9 December 2004

The genome of the nucleorhabdovirus maize fine streak virus (MFSV) consists of 13,782 nucleotides of nonsegmented, negative-sense, single-stranded RNA. The antigenomic strand consisted of seven open reading frames (ORFs), and transcripts of all ORFs were detected in infected plants. ORF1, ORF6, and ORF7 had significant similarities to the nucleocapsid protein (N), glycoprotein (G), and polymerase (L) genes of other rhabdoviruses, respectively, whereas the ORF2, ORF3, ORF4, and ORF5 proteins had no significant similarities. The N (ORF1), ORF4, and ORF5 proteins localized to nuclei, consistent with the presence of nuclear localization signals (NLSs) in these proteins. ORF5 likely encodes the matrix protein (M), based on its size, the position of its NLS, and the localization of fluorescent protein fusions to the nucleus. ORF2 probably encodes the phosphoprotein (P) because, like the P protein of *Sonchus yellow net virus* (SYNV), it was spread throughout the cell when expressed alone but was relocalized to a subnuclear locus when coexpressed with the MFSV N protein. Unexpectedly, coexpression of the MFSV N and P proteins, but not the orthologous proteins of SYNV, resulted in accumulations of both proteins in the nucleolus. The N and P protein relocalization was specific to cognate proteins of each virus. The subcellular localizations of the MFSV ORF3 and ORF4 proteins were distinct from that of the SYNV sc4 protein, suggesting different functions. To our knowledge, this is the first comparative study of the cellular localizations of plant rhabdoviral proteins. This study indicated that plant rhabdoviruses are diverse in genome sequence and viral protein interactions.

Members of the family *Rhabdoviridae* have a broad host range, including humans, livestock, plants, and insects. Six genera of rhabdoviruses have been described (40). The four genera of animal-infecting rhabdoviruses (*Vesiculovirus*, *Ephemerovirus*, *Lyssavirus*, and *Novirhabdovirus*) include the livestock pathogens *Vesicular stomatitis Indiana virus* (VSIV), *Vesicular stomatitis New Jersey virus* (VSNJV), and *Bovine ephemeral fever virus*; the human pathogen *Rabies virus* (RABV); and the fish pathogen *Infectious hematopoietic necrosis virus*. The two genera of plant rhabdoviruses are *Cytorhabdovirus* (type species, *Lettuce necrotic yellows virus* [LNYV]) and *Nucleorhabdovirus* (type species, *Potato yellow dwarf virus*). The viruses that cause rabies and fish diseases appear to be confined to vertebrate hosts, whereas vesiculo-, ephemero-, cyto-, and nucleorhabdoviruses are transmitted to their vertebrate or plant hosts by insects (20, 35). Plant rhabdoviruses are particularly interesting because they are able to replicate and systemically spread in very divergent hosts: plants and insects.

Generally, a rhabdovirus virion is composed of a lipid envelope derived from host membranes and a ribonucleocapsid core consisting of a nonsegmented, negative-sense, single-stranded RNA bound to complexes of nucleocapsid protein (N), phosphoprotein (P), and polymerase (L) (35). The glycoprotein (G) protrudes from the exterior of the lipid envelope, and the matrix protein (M) connects the envelope to the ribonucleocapsid core (35). VSIV and VSNJV have the simplest genomes, encoding just the five structural proteins of the virion in the gene order 3′-*N*-*P*-*M*-*G*-*L*-5′, whereas the genomes of other rhabdoviruses harbor additional genes (18, 26, 30, 39, 42).

Although >70 plant rhabdoviruses have been described, the genomes of only a few plant rhabdoviruses have been sequenced to completion, including *Northern cereal mosaic virus* (NCMV), *Rice yellow stunt virus* (RYSV), and *Sonchus yellow net virus* (SYNV) (4, 5, 6, 9, 11, 17, 19, 21, 28, 29, 36, 39, 41, 43, 44, 45). The nucleorhabdovirus SYNV is presently the most extensively characterized plant-infecting rhabdovirus (22). In planta subcellular localization studies of fluorescent-protein fusions provided an indication of the function and protein-protein interactions of viral proteins of SYNV (13). The SYNV N and M proteins both target the plant cell nucleus when expressed individually, whereas the SYNV P and sc4 proteins do not (13). However, the SYNV P protein targets subnuclear locales when coexpressed with the SYNV N protein, suggesting that the N and P proteins interact with each other in SYNV-infected plants (12, 13). The SYNV *sc4* gene, located between the *P* and *M* genes, encodes a membrane-associated protein that may be involved in viral cell-to-cell movement in plants (31, 36).

Maize fine streak virus (MFSV) was first reported in maize fields in southwestern Georgia in 1999 and was described as a new plant nucleorhabdovirus (34). The symptoms caused by MFSV include dwarfing and fine chlorotic streaks along intermediate and small veins (34). MFSV is transmitted by the leafhopper *Graminella nigrifrons* and is not transmissible by

* Corresponding author. Mailing address: Department of Entomology, The Ohio State University-Ohio Agricultural Research and Development Center (OARDC), 1680 Madison Ave., Wooster, OH 44691. Phone: (330) 263-3730. Fax: (330) 263-3686. E-mail: hogenhout.1@osu.edu.

rub inoculation of maize leaves but can be mechanically transmitted by vascular puncture inoculation (VPI) (20, 34). Like those of other rhabdoviruses, the MFSV virion is a bacilliform particle measuring 231 by 71 nm with a lipid envelope, and its genome consists of a nonsegmented, negative-sense, single-stranded RNA (34, 40). Purified preparations of MFSV contain three abundant proteins corresponding to the major rhabdovirus structural proteins: the G protein (82 kDa), N protein (50 kDa), and M protein (32 kDa) (34).

To define MFSV genes and to begin to characterize their functions, we determined the complete genomic sequence of the virus and investigated virus gene expression in infected maize. We showed for the first time the localization of coexpressed rhabdoviral N and P proteins in the nucleolus of plant cells and that the N and P proteins of MFSV and SYNV specifically interact with each other and not with the orthologous proteins of another rhabdovirus. Further, we demonstrated that the MFSV ORF3 and ORF4 proteins had different subcellular localizations than the SYNV sc4 protein.

MATERIALS AND METHODS

Virus maintenance and purification. MFSV from Georgia was maintained in maize seedlings by serial inoculations with viruliferous insect vectors (*G. nigrifrons*) or by VPI (27, 34). The virus was purified from maize leaf laminar tissue collected 26 to 40 days after VPI or vector inoculation, as previously described (34).

MFSV genomic RNA extraction and library construction. For initial cDNA library construction, virus genomic RNA was extracted using a previously described protocol (34). For all other applications (reverse transcription [RT]-PCR, 3′ rapid amplification of cDNA ends (RACE), 5′ RACE, and RNA ligase-mediated (RLM) RACE), genomic RNA was extracted from virus pellet suspensions using a ToTALLY RNA isolation kit (Ambion, Austin, Tex.) following the manufacturer's instructions.

The cDNA synthesis of the MFSV genomic RNA using random hexamers was carried out with the Superscript Choice system (Invitrogen Corp., Carlsbad, Calif.) according to the manufacturer's instructions. The cDNAs were ligated into the EcoRI-digested, phosphatase-treated pGEM4Z vector (Promega Corp., Madison, Wis.) or the pZeroAmp vector (T. Meulia, unpublished results) and transformed into *Escherichia coli* TOP10 cells (Invitrogen Corp.). Twelve clones (G2A, G2C, G3A, G3B, G4C, G5C, G6A, G9B, Z6B, Z11B, Z12B, and Z15B) carrying inserts larger than 1 kb that hybridized with viral RNA were selected for sequence analysis.

Regions of the MFSV genomic RNA not represented by clones were amplified using RT-PCR with primers flanking the missing sequence. RT-PCR was carried out using a Platinum RT-PCR kit (Invitrogen Corp.). RT-PCR products for the 3′ end of the MFSV genome (GAU3′) and MFSV4 (Fig. 1) were ligated into the pCR-Blunt II-TOPO vector (Invitrogen Corp.) for sequencing. Three other RT-PCR products, MFSV5, MFSV6, and MFSV7 (Fig. 1) were sequenced directly, without prior cloning.

MFSV genome sequencing and sequence analysis. Sequencing was carried out in 550- to 700-bp segments by primer walking using a 3700 DNA Sequence Analyzer and BigDye Terminator Cycle Sequencing chemistry (Applied Biosystems, Inc., Foster City, Calif.) according to the supplier's instructions. Base calling was done with MacPHRED-MacPHRAP (CodonCode Corp., Dedham, Mass.), and sequences were assembled by Sequencher (Gene Codes Corp., Ann Arbor, Mich.).

ORFs were identified with MacVector version 6.5 (Accelrys, San Diego, Calif.). Putative MFSV protein sequences were compared to the National Center for Biotechnology Information (NCBI) GenBank database by BLASTP search to identify sequence similarity to other known proteins. Protein sequences were searched for domains and motifs, including transmembrane domains (TMHMM version 2.0 [http://www.cbs.dtu.dk/services/TMHMM/]) (37), N-terminal signal peptides (SignalP version 3.0 [http://www.cbs.dtu.dk/services/SignalP/]) (3), nuclear localization signals (NLSs) (PROSITE [http://us.expasy.org/prosite/] [8] and PredictNLS [http://cubic.bioc.columbia.edu/predictNLS/] [7]), and glycosylation sites (PROSITE).

Sequencing of the 3′ and 5′ ends of the MFSV genome. The terminal sequences of MFSV were identified by RACE. The viral 5′ trailer region was determined by both 5′ RACE (Invitrogen Corp.) and RLM-RACE (Ambion) following the manufacturers' instructions. For 5′ RACE, the cDNA of the MFSV genomic RNA was synthesized using a gene-specific primer, 5′ RACE GSP1 (5′-AAATCTCTGTTGAGCC-3′), and tailed with dCTP using terminal deoxynucleotidyl transferase. The first amplification was carried out with the abridged anchor primer and a 5′ RACE GSP2 primer (5′-GGTCCATTGCAGAGAGA TCAAC-3′). Nested amplification used the abridged universal amplification primer (AUAP) and a 5′ RACE GSP3 primer (5′-CTATCCTATCAGATCCC ATAATGC-3′). For RLM-RACE, a 45-bp 5′ RACE adapter was added to the MFSV genomic RNA, and then the cDNA was synthesized using random decamers. The first amplification was carried out with the 5′ RACE outer primer and the 5′ RACE GSP2 primer. Nested amplification used the 5′ RACE inner primer and the 5′ RACE GSP3 primer.

The viral 3′ leader region was determined by 3′ RACE (Invitrogen Corp.). The MFSV genomic RNA was tailed with ATP using the Poly(A) Tailing kit (Ambion), and cDNA was synthesized using the oligo(dT)-containing adapter primer. The first amplification was carried out with the AUAP and a 3′ RACE GSP1 primer (5′-CTAAGAATGTCAGGAATAGGTCCTG-3′), and nested amplification was done with the AUAP and a 3′ RACE GSP2 primer (5′-CACCATA GGATAGACATGCATTCC-3′). The 5′ RACE and 3′ RACE products were ligated into the pGEM-T Easy vector (Promega Corp.) for sequencing.

Rhabdovirus nucleotide sequences used for interspecies comparison were obtained from the genome sequences in the NCBI GenBank database for the following viruses: SYNV (NC 001615), RYSV (NC 003746), NCMV (NC 002251), LNYV (L24365 and L24364) (42), VSIV (NC 001560), and RABV (NC 001542).

Characterization of transcription start sites of the MFSV *G* and *L* genes. The transcription start sites of the MFSV *G* and *L* genes were identified by RLM-RACE. Total RNA from infected maize leaves was extracted with a ToTALLY RNA isolation kit. Subsequently, mRNA was isolated from the total RNA preparation using a Dynabead mRNA DIRECT kit (Dynal ASA, Oslo, Norway) following the manufacturer's instructions. The cDNA was synthesized from the adapter-ligated mRNA with random decamers. The first amplification was carried out with either the 5′ RACE outer primer and a G outer primer (5′-GTA CTTAGTGGCAATGATGGTGTC-3′) or the 5′ RACE outer primer and an L outer primer (5′-GCTTGTAACAGTGCCCACATATC-3′). Nested amplification was carried out with either the 5′ RACE inner primer and a G inner primer (5′-CGATTATCAGTGTCGAGTTGTTC-3′) or the 5′ RACE inner primer and an L inner primer (5′-GTATGTCCCCCATGAGATAGTC-3′). The RLM-RACE products were ligated into the pGEM-T Easy vector for sequencing.

Northern blot hybridization analysis. Total RNA (10 μg) from infected and healthy maize was denatured using glyoxal sample loading dye (Ambion) and separated on a 1.2% BPTE {100 mM PIPES [piperazine-*N*,*N*′-bis(2-ethanesulfonic acid)], 300 mM bis-Tris, 10 mM EDTA, pH 6.5} agarose gel, transferred to a positively charged BrightStar-Plus nylon membrane (Ambion) with 20× SSC (3 M NaCl, 0.3 M sodium citrate, pH 7.0), and cross-linked to the membrane by exposure to UV light (UV Transilluminator; Fisher Scientific, Pittsburgh, Pa.) for 2 min. Probes were prepared by PCR amplification of DNA fragments corresponding to each gene from the cDNA clones and subsequent incorporation of [^{32}P]dCTP (Amersham Biosciences Corp., Piscataway, N.J.) (10). Hybridization of probes to Northern blots was carried out as previously described (32). Northern blots were washed three times for 10 min each in 2× SSC and 0.1% sodium dodecyl sulfate and four times for 10 min each in 0.1× SSC and 0.1% sodium dodecyl sulfate at 65°C and then exposed to Storage Phosphor Screen (Molecular Dynamics, Sunnyvale, Calif.) for 24 h. Images were captured using ImageQuant software (Molecular Dynamics), converted to TIFF for export, and processed in Photoshop version 7.0 (Adobe, San Jose, Calif.).

Construction of pGD derivatives for in planta subcellular localization. Construction of the binary pGDG and pGDR vectors, the pGDG construct for in planta synthesis of the *Arabidopsis thaliana* Fib1 (AtFib1)-green fluorescent protein (GFP), GFP-SYNV N, and the pGDR construct for in planta synthesis of DsRed-SYNV P were described previously (13). The pGDB and pGDY vectors were constructed by modification of pGD (13). The cyan fluorescent protein (CFP) and yellow fluorescent protein (YFP) genes were amplified from pECFP-C1 and pEYFP-C1 (BD Biosciences, Palo Alto, Calif.), respectively. The PCR products were subcloned into the pGD vectors in a manner that reconstituted the multiple cloning site of pGD, since BglII, HindIII, and XhoI restriction sites were incorporated into the 3′ ends of the PCR products. The CFP and YFP genes in the new vectors were verified by DNA sequencing and expression in plant cells. The complete predicted MFSV ORFs (i.e., from the putative start codon to the first stop codon) were expressed as fusions to the C termini of autofluorescent proteins. The MFSV ORFs were amplified from corresponding cDNA clones by PCR, and primers with overhanging restriction sites were

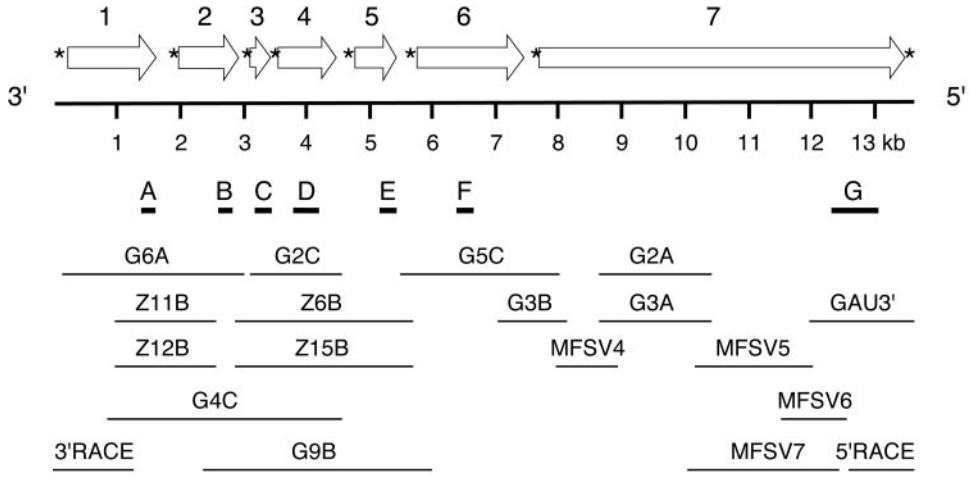

FIG. 1. Schematic diagram of the MFSV genome organization. The open reading frames (block arrows) are derived from the antigenomic sequence. The asterisks indicate gene junctions (Fig. 3). Bold lines indicate locations of probes A, B, C, D, E, F, and G used for Northern blot hybridization of mRNAs of ORF1, -2, -3, -4, -5, -6, and -7, respectively (Fig. 5).

introduced to facilitate directional cloning into the binary vector pGDB, pGDG, pGDR, or pGDY as previously described (13). PCR was performed using the high-fidelity DynazymeEXT polymerase (Finnzymes, Espoo, Finland). PCR products were cloned directly into the pCRII vector (Invitrogen Corp.) using topoisomerase-mediated cloning. The DNA sequences of the full-length clones for the MFSV *N*, *P*, *3*, *4*, and *M* genes in pGD derivatives were verified prior to transformation into *Agrobacterium tumefaciens* strain C58C1.

Agroinfiltration procedures. *A. tumefaciens* was infiltrated into leaves of *Nicotiana benthamiana* as previously described (13). Briefly, suspensions of transformed C58C1 agrobacteria were adjusted to an optical density at 600 nm of 0.6 in agroinfiltration buffer (10 mM $MgCl_2$, 10 mM MES [morpholineethanesulfonic acid], pH 5.6), and acetosyringone was added to a final concentration of 150 μM (13). An agrobacterial suspension was infiltrated into the mesophyll of leaves using a 1-ml disposable syringe. Following infiltration, the leaves were examined by epifluorescence microscopy between 40 and 90 h postinfiltration.

DAPI staining of plant nuclei. DAPI (4′-6-diamidino-2-phenylindole dihydrochloride; 15 μg/ml) in agroinfiltration buffer was infiltrated into leaves as described by Goodin et al. (13). Following infiltration, the plants were incubated in the dark for 1 to 2 h before examination of leaf sections by epifluorescence microscopy.

Epifluorescence microscopy. Epifluorescence micrographs were acquired using an Axiocam MR monochromatic digital camera mounted on a motorized Axioplan2 microscope (Carl Zeiss Microimaging Inc., Thornwood, N.Y.). Camera and microscope settings were controlled by Axiovision software version 4.1. False colors for differentiating DAPI, CFP, GFP, and DsRed2 fluorescences were assigned using color settings in the Axiovision software. Filter sets that permitted viewing of the relevant fluorescences were purchased from Chroma Technology Corp. (Rockingham, Vt.) and included the following filter sets. (i) Filter set 31001 for viewing GFP; this set consisted of a D470/40× excitation (Ex) filter, a 505 DCLP dichroic, and a D540/40× emission (Em) filter. (ii) Filter set 31000 was used for viewing DAPI-stained nuclei. This set consisted of a D360/40× Ex filter, a 400 DCLP dichroic, and a D460/50 M Em filter. (iii) Filter set 310044 V2, used for capturing CFP fluorescence, consisted of a D436/20× Ex filter, a 455DCLP dichroic, and a D480/40 M Ex filter. (iv) YFP fluorescence was viewed using a 41028 filter set that consisted of an HQ500/20× Ex filter, a Q5151LP dichroic, and a HQ535/30 M Em filter. (v) For viewing fluorescence from DsRed2, a 41035 filter set, consisting of a HQ546/12× Ex filter, a Q560LP dichroic, and a HQ650/75 M Em filter, was used. The lenses used in this study included the Plan Neofluar 10×/NA 0.3; the Plan Neofluar 25×/NA 0.8 multiple immersion lens, used primarily in the water immersion setting; and a Plan Apochromat 100×/NA 1.4 oil immersion lens. Sections of plant tissue were mounted in water on standard glass slides and covered with no. 1 glass coverslips (Corning Inc., Corning, N.Y.). Leaves were mounted so that the abaxial surface was viewed. Micrographs were exported from the Axiovision software as TIFF files. All subsequent cropping and image manipulations were carried out in Photoshop version 7.0 (Adobe Systems Inc., San Jose, Calif.) and Canvas version 8.0 (Deneba Software, Miami, Fla.).

Confocal laser scanning microscopy. Confocal laser scanning micrographs were acquired on a TCS SP2-AOBS microscope (Leica Microsystems, Bannockburn, Ill.). GFP variants were excited simultaneously using the 488-nm laser line. Fluorescence emissions from CFP, GFP, and YFP could be distinguished using the spectral imaging capability provided by the prism spectrophotometer of the microscope. The ability to unambiguously differentiate these three fluors when coexpressed in leaf epidermal cells allowed assignment of the subnuclear locales in which the N and P proteins accumulate.

Nucleotide sequence accession number. The sequence of the MFSV genome was deposited in GenBank under accession number NC 005974.

RESULTS

Nucleotide sequence of MFSV. The MFSV genome sequence was obtained by assembling sequences derived from the overlapping sequences of 12 randomly primed cDNA clones, five RT-PCR products, and two RACE products (Fig. 1). The MFSV genome consisted of 13,782 nucleotides (nt) and seven ORFs on the antigenomic strand.

The sequence of the 3′ end of the MFSV genome was determined by 3′ RACE, and that of the 5′ end was deter-

```
MFSV   3' UGUGUGGUUUUUCCCACUGCGUAGGUUCUU....
          |||||    ||||    |||||||||   |
       5' ACACAGGCAAAAAAAUGACGCAUCACAACU....

SYNV   3' UCUCUGUCUUUGAGUCUUUUAUGUUAGUGG....
          |||||||  ||  ||||||| |   |   |    |
       5' AGAGACAAAAGCUCAGAACAAUCCCUAUAC....

RYSV   3' UGUGGUGGUCUAUGUAAGACAUUUAUCAAA....
          ||||||||| || ||          ||    |
       5' ACACCACCAUAUCCAAAGCCGCCAUGUGUG....

NCMV   3' GUGCUGGU_CACUAGCUUGUUGGACUUAGUA....
            ||||  ||  ||||  ||  ||      | |
       5'  ACGAUCAAGUGAGCGGACCUGGUAAGCAUC....

LNYV   3' AAUGCCUGUUAUUAUCUUCUUUUUUUAGUUCA....
             ||||||  ||||||  ||   |||||  ||  |  |
       5'    ACGGACGAUAAUAAAAUCAAAAAGUCCAAU....
```

FIG. 2. Sequences of the 3′ and 5′ termini of plant rhabdovirus genomes. Sequences are shown in the genomic sense. Vertical lines indicate complementary nucleotides between leader and trailer sequences. Overhangs in leader sequences are underlined.

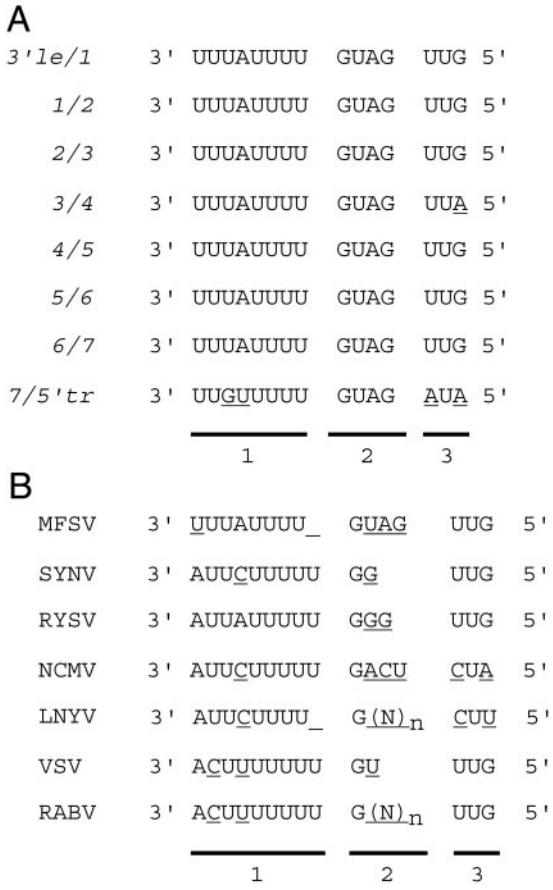

FIG. 3. Comparison of rhabdovirus gene junctions. (A) Gene junctions of the MFSV genome. The three motifs are indicated, corresponding to the 3′ ends of the mRNAs (column 1), intergenic sequences (column 2), and the 5′ ends of the mRNAs (column 3). (B) Consensus sequences of gene junctions of plant and animal rhabdoviruses. All sequences are presented in genomic sense in the 3′-to-5′ orientation, and nucleotide differences are underlined. Abbreviations: 3′ le, 3′ leader sequence; 5′ tr, 5′ trailer sequence; $(N)_n$, variable number of nucleotides.

mined by 5′ RACE and RLM-RACE. The 3′ RACE PCR products were cloned, and inserts of all six clones were identical, indicating that the 3′ end of the MFSV genome was 3′-UGUGUGGUUUUUCCCACUGC · · · -5′. The sequences of inserts of four 5′ RACE and RLM-RACE clones were identical, indicating that the 5′ end of the MFSV genome was 3′- · · · GCAGUAAAAAAACGGACACA-5′. Identical 5′- and 3′-end sequences using either poly(A) or poly(C) adapters were obtained at the University of Wisconsin (P. Flanary and T. L. German, personal communication). These results led to the conclusion that the MFSV genomic RNA had a 184-nt 3′ leader region preceding the leader-*N* intergenic sequence and a 145-nt 5′ trailer region following the *L*-trailer intergenic sequence.

Comparison of the 3′ and 5′ ends of the MFSV genomic RNA revealed that 19 of 30 nucleotides were complementary and might give rise to a putative panhandle structure (Fig. 2). Similar structures were reported for SYNV, LNYV, and NCMV (6, 39, 42). In addition, the first 30 nt of the 3′ leader

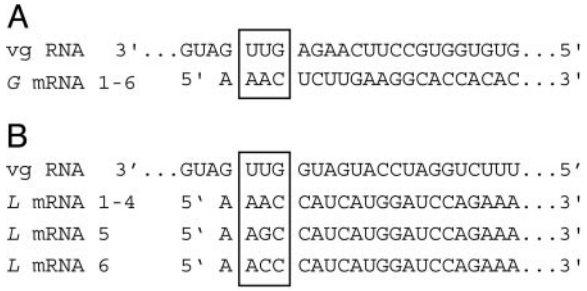

FIG. 4. RLM-RACE of the MFSV *G* and *L* mRNAs. The sequences of six clones, each derived from the *G* gene and *L* gene mRNAs, were determined. Nucleotides of mRNAs complementary to the transcription start sites in the conserved gene junction sequences of the viral genome (vg) are boxed.

sequence had a high U residue content (47%), similar to those described for SYNV (53%), RYSV (37%), NCMV (37%), and LNYV (60%). Although the plant rhabdoviruses share complementarity of their 3′ and 5′ ends and have similar nucleotide biases, these sequences did not have significant sequence identity among rhabdoviruses (Fig. 2).

Gene junctions of the MFSV genome. The MFSV ORFs were separated by gene junctions with the consensus sequence 3′-UUUAUUUUGUAGUUG-5′(Fig. 3A). This sequence was broadly conserved among plant and animal rhabdoviruses (Fig. 3B) and was divided into three distinct motifs: the sequences corresponding to the 3′ ends of mRNAs, the intergenic sequences, and the sequences corresponding to the 5′ ends of mRNAs (35) (Fig. 3). The corresponding sequences of MFSV mRNA 3′ ends were A/U rich and 8 nucleotides in length, and only the ORF7-5′ trailer junction had 2 nucleotide differences from the consensus sequence. The intergenic sequence GAUG was conserved in all gene junctions of MFSV; however, this sequence was not conserved among rhabdoviruses (Fig. 3B). The transcription start site consisted of 3 nucleotides, and only the ORF4 mRNA start site had a single-nucleotide change relative to the consensus sequence, UUG. The MFSV transcription start site was identical to those of other rhabdoviruses (SYNV, RYSV, VSIV, and RABV), except for the two cytorhabdoviruses NCMV and LNYV (Fig. 3B).

Transcription start sites of the MFSV *G* and *L* genes. RLM-RACE was used to confirm the sequences of the putative transcription start sites for the MFSV *G* and *L* genes (Fig. 4). The sequences of six RLM-RACE products for the *G* gene were identical (Fig. 4A). The sequences of four RLM-RACE products for the *L* gene were identical, while the sequences of two others differed from these at position 3 (Fig. 4B). These data are consistent with the putative UUG transcription start sites identified in Fig. 3A. However, the 5′ ends of transcripts contained a nucleotide A that does not correspond to the viral genomic sequence (Fig. 4). Whether the single-nucleotide change at the third nucleotide found in two *L* gene RLM-RACE clones was due to true variability in the *L* gene mRNAs is not known.

Analysis of the MFSV ORF sequences. The predicted proteins encoded by the seven MFSV ORFs were examined for sequence similarity to other proteins in the NCBI GenBank nonredundant database using BLASTP. The deduced protein

TABLE 1. Features of encoded proteins of MFSV genome

ORF no.	Calculated mass (kDa)	TM (position in protein)[a]	NLS (position in protein)[a]	Putative function
1	51.6	ND	+ (C-term)	Nucleocapsid protein (N)
2	38.4	ND	ND	Phosphoprotein (P)
3	10.7	ND	ND	Unknown
4	37.2	ND	+ (N-term)	Unknown
5	28.5	ND	+ (C-term)	Matrix protein (M)
6	67.0	+ (C-term)	ND	Glycoprotein (G)
7	223.5	ND	ND	Polymerase (L)

[a] TM, transmembrane domain; ND, not detected; N-term, N-terminal half of protein; C-term, C-terminal half of protein; +, present.

sequence of ORF1 had significant similarity to the N proteins of RYSV (expected [E] value = $8e^{-21}$), SYNV (E value = $1e^{-19}$), and NCMV (E value = $5e^{-6}$). The ORF6 protein sequence had significant similarity to those of the G proteins of RYSV (E value = $5e^{-22}$) and SYNV (E value = $1e^{-16}$), and the ORF7 protein sequence had significant similarity to those of the L proteins of SYNV (E value = 0.0), RYSV (E value = 0.0), and other nonsegmented, negative-sense RNA viruses. Thus, based on sequence similarity, MFSV ORF1, ORF6, and ORF7 likely encode the N, G, and L proteins, respectively. The ORF2, ORF3, ORF4, and ORF5 protein sequences did not show any significant similarities to other rhabdovirus proteins or other sequences in GenBank.

The protein sequences of MFSV and other nucleorhabdoviruses were searched for domains and motifs, including NLSs, glycosylation sites, N-terminal signal peptides, and transmembrane domains. Putative NLSs were found at amino acid positions 436 to 452 (KRSSDGTGNVSKKKSRK) of the N protein, at positions 17 to 33 (RKALTKASKALFKGKIK) of the ORF4 protein, and at positions 195 to 211 (KKEDKAEKAT TEKRKRQ) of the ORF5 protein, whereas no NLSs were identified in the MFSV ORF2, ORF3, G, and L proteins (Table 1). The SYNV N and M and RYSV N proteins also had putative NLSs in the carboxyl regions, but no putative NLS was identified in the RYSV M protein (33).

Similar to other rhabdovirus G proteins, the putative MFSV G protein apparently has abundant glycosylation signals. Eight potential glycosylation signals (N-[P]-S/T-[P]-) were located at amino acid positions 64 to 67, 131 to 134, 132 to 135, 139 to 142, 204 to 207, 325 to 328, 438 to 441, and 494 to 497. The MFSV G protein also had an N-terminal signal peptide sequence (MMARLVPCFTLALLLHLTEC) and a putative cleavage site (C/A) between amino acid positions 20 and 21. Furthermore, a transmembrane domain (FIIKLVIGFTVGT IMLYISWIII) was identified at amino acid positions 529 to 551. Other predicted proteins of MFSV did not have abundant glycosylation sites, signal peptide sequences, or transmembrane domains.

Detection of MFSV ORF transcripts in plants. To test whether all the identified ORFs in the MFSV genome are transcribed, Northern blots of total RNAs from healthy and MFSV-infected maize were hybridized with probes corresponding to each ORF (Fig. 1). Transcripts of expected sizes that corresponded to each of the seven ORFs were detected in MFSV-infected maize (Fig. 5), whereas no hybridization occurred with RNA from healthy maize (data not shown). Several RNAs hybridized to the ORF7 probe, with the size of the largest matching the expected size of the ORF7 transcript (Fig. 5A, lane L). The predicted length of gene *3* is 357 nt, and a transcript of ~400 bp hybridized to the ORF3 probe (Fig. 5A, lane 3). The predicted length of gene *4* is 1,185 nt, and a transcript of ~1,200 bp hybridized to the ORF4 probe (Fig. 5A, lane 4). To exclude the possibility of RNA degradation, a blot that was hybridized with the ORF4 probe was subsequently probed with the ORF3 probe. As expected, the resulting blot showed two distinct hybridized bands (Fig. 5B). These results demonstrated that seven distinct transcripts were present in MFSV-infected maize and that these transcripts corresponded to the seven putative genes identified in the MFSV genome.

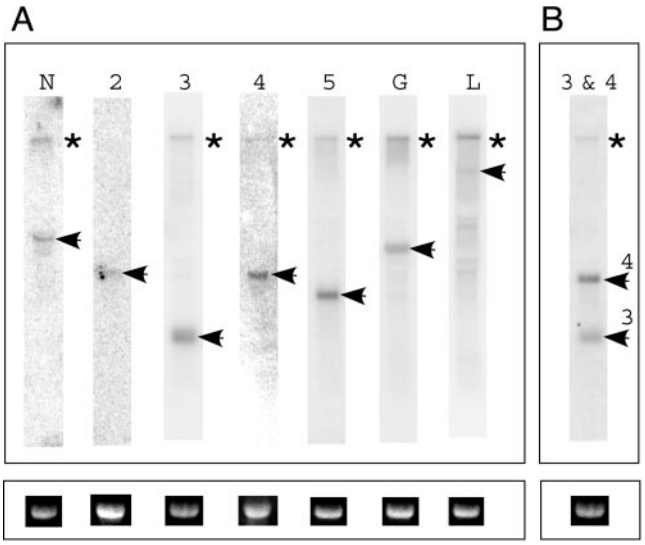

FIG. 5. Detection of MFSV gene transcripts in infected maize by Northern blot analysis. (A) Blots of total RNA isolated from healthy (data not shown) or MFSV-infected maize hybridized to probes A, B, C, D, E, F, and G, which are located within the MFSV *N*, *2*, *3*, *4*, *5*, *G*, and *L* genes, respectively. (B) Blot hybridized to probe D and subsequently to probe C. Figure 1 shows the localizations of the probes. The asterisks indicate migration of the genomic RNA of MFSV, and the arrows indicate hybridization to mRNAs. Gel images of 25S rRNA were used as loading controls (below).

Subcellular localization of the MFSV proteins. NLSs were identified in three of the seven MFSV ORFs, and nuclear localization was demonstrated for the SYNV N and M proteins (13). To determine the subcellular localization of the MFSV proteins, we used in planta localization and colocalization of fluorescent-protein fusions. Full-length ORF sequences were introduced into binary pGD derivatives for *A. tumefaciens*-mediated agroinfiltration of *N. benthamiana* leaves (13) and subsequent in planta production of MFSV proteins fused at the N terminus to CFP, YFP, and GFP.

Agroinfiltration of fluorescent-protein fusions of MFSV N, ORF2, ORF3, ORF4, and ORF5 proteins showed that CFP-MFSV N, GFP-MFSV 4, and GFP-MFSV 5 accumulated in the nucleus (Fig. 6 and 7B and C), whereas YFP-MFSV 2 spread throughout the cell (Fig. 6) and YFP-MFSV 3 accumulated in punctate loci in the cytoplasm (Fig. 7A). These results

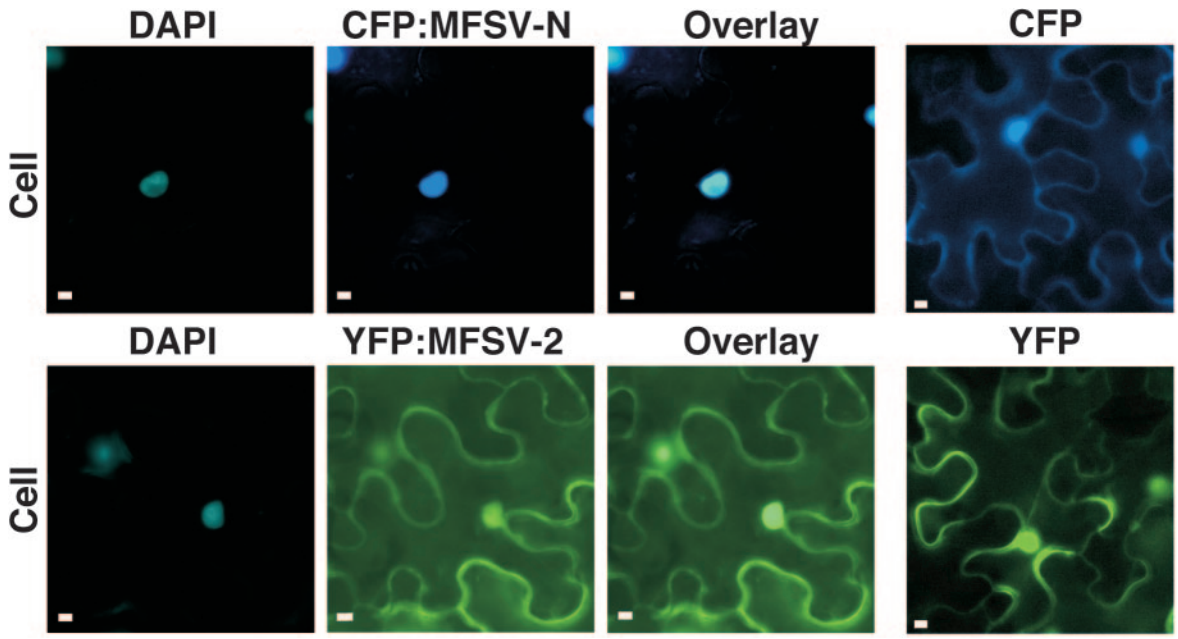

FIG. 6. Epifluorescence microgaphs of subcellular localizations of fluorescent-protein fusions of the MFSV N and ORF2 proteins. The DNA selective dye DAPI was used to determine the positions of nuclei in plant cells. Infiltrations of unfused CFP and YFP were included as negative controls. Cellular views of localizations of CFP-MFSV N to the nucleus (top row), and YFP-MFSV 2 throughout the cell (bottom row) are shown. Bars = 5 μm.

were consistent with the prediction of NLSs in the MFSV N, ORF4, and ORF5 proteins.

When leaves were coinfiltrated with mixtures of C58C1 agrobacteria harboring CFP-MFSV N and YFP-MFSV 2 fusions, both fusions colocalized to the subnucleus (Fig. 8A). However, unlike the SYNV N and P proteins, the MFSV N and ORF2 proteins localized to the nucleolus (Fig. 8A). To confirm the nucleolar localization, we coexpressed CFP-MFSV N and YFP-MFSV 2 with the AtFib1-GFP that localizes to the nucleolus in *A. thaliana* and *N. benthamiana* epidermal cells (2, 13). This result confirmed that CFP-MFSV N and YFP-MFSV 2 targeted the same subnuclear locale as AtFib1-GFP, which is in the nucleolus (Fig. 8B).

Finally, we determined whether coinfiltration of fluorescent-protein fusions of the MFSV N protein and the SYNV P protein allowed redirection of cytosolic SYNV P protein to the subnuclear locale, similar to coexpression of the SYNV N and P proteins. Coinfiltrated CFP-MFSV N and DsRed-SYNV P did not interact to target a subnuclear locale but looked very similar to DsRed-SYNV P infiltrated alone (Fig. 9). Similar results were obtained when GFP-SYNV N was coinfiltrated with YFP-MFSV 2 (Fig. 9). These data suggest that the interaction of N and P proteins leading to subnuclear targeting is virus specific.

DISCUSSION

We have mapped and sequenced the complete genome of the leafhopper-transmitted maize pathogen MFSV and showed that all seven genes included in its genome are expressed during infection of maize. Furthermore, in planta subcellular localization studies of fluorescent-protein fusions showed that the MFSV N, ORF4, and ORF5 proteins were targeted to the nuclei and that coinfiltrated MFSV N and ORF2 proteins interacted, resulting in targeting of both proteins to the nucleolus. We also showed that the nuclear targeting of coinfiltrated N and P proteins was virus specific and that the protein products of the two additional genes (*3* and *4*) of MFSV had different subcellular localizations than the SYNV sc4 protein.

Assignment of functions for the MFSV N (ORF1), G (ORF6), and L (ORF7) proteins could be made largely on the basis of sequence similarities to SYNV genes and proteins. However, nucleotide and deduced protein sequences of ORF2, ORF3, ORF4, and ORF5 showed few similarities to other rhabdovirus genes or sequences in GenBank. We used in planta subcellular localization of fluorescent-protein fusions, a useful technique in protein subcellular targeting studies and for elucidation of protein function (13, 15, 38), to begin to define the functions of the MFSV ORFs.

The most likely gene order of the MFSV genome is 3′-*N-P-3-4-M-G-L*-5′. Sequence analysis and in planta localization results suggest that ORF2 of MFSV encodes the P protein because (i) *P* is located adjacent to *N* in all rhabdoviruses sequenced so far, (ii) the predicted size of the ORF2 protein is similar to those of P proteins of other rhabdoviruses, and (iii) similar to the SYNV N and P proteins (13), coinfiltration of the MFSV N protein with the MFSV ORF2 protein resulted in nucleolar localization of both proteins, whereas the MFSV N protein targeted the whole nucleus and the MFSV ORF2 protein spread throughout the cell when the proteins were infiltrated alone. For ORF5 of MFSV, sequence analysis and in planta localization results indicate that this ORF probably encodes the M protein because (i) the position of the NLS and

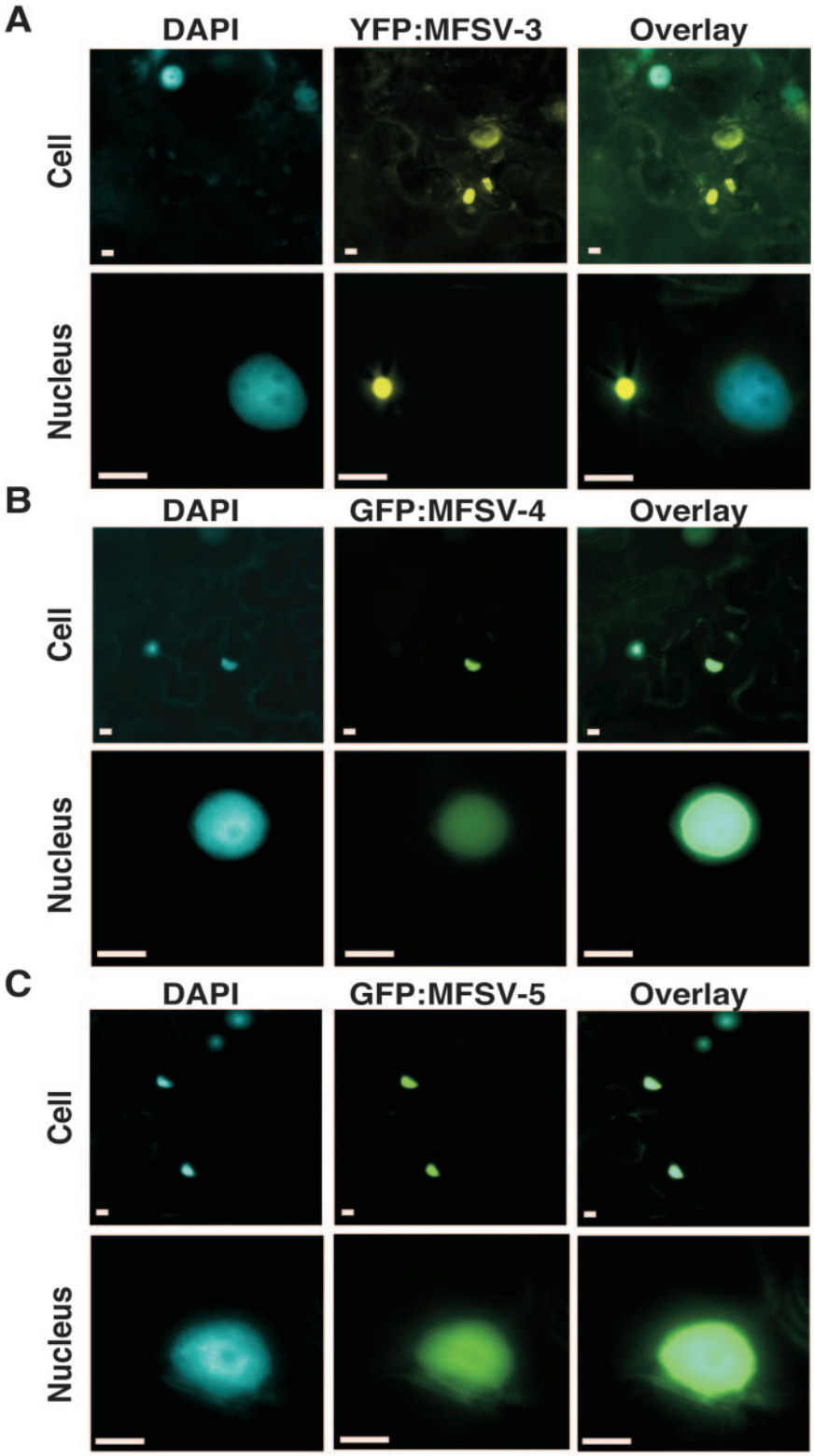

FIG. 7. Epifluorescence micrographs of subcellular localizations of fluorescent-protein fusions of the MFSV ORF3, ORF4, and ORF5 proteins in the cellular (top rows) and nuclear (bottom rows) views. The DNA selective dye DAPI was used to determine the positions of nuclei in plant cells. (A) Accumulation of YFP-MFSV 3 in punctate loci in the plant cell cytoplasm. (B) Nuclear localization of GFP-MFSV 4. (C) Nuclear localization of GFP-MFSV 5. Bars = 5 μm.

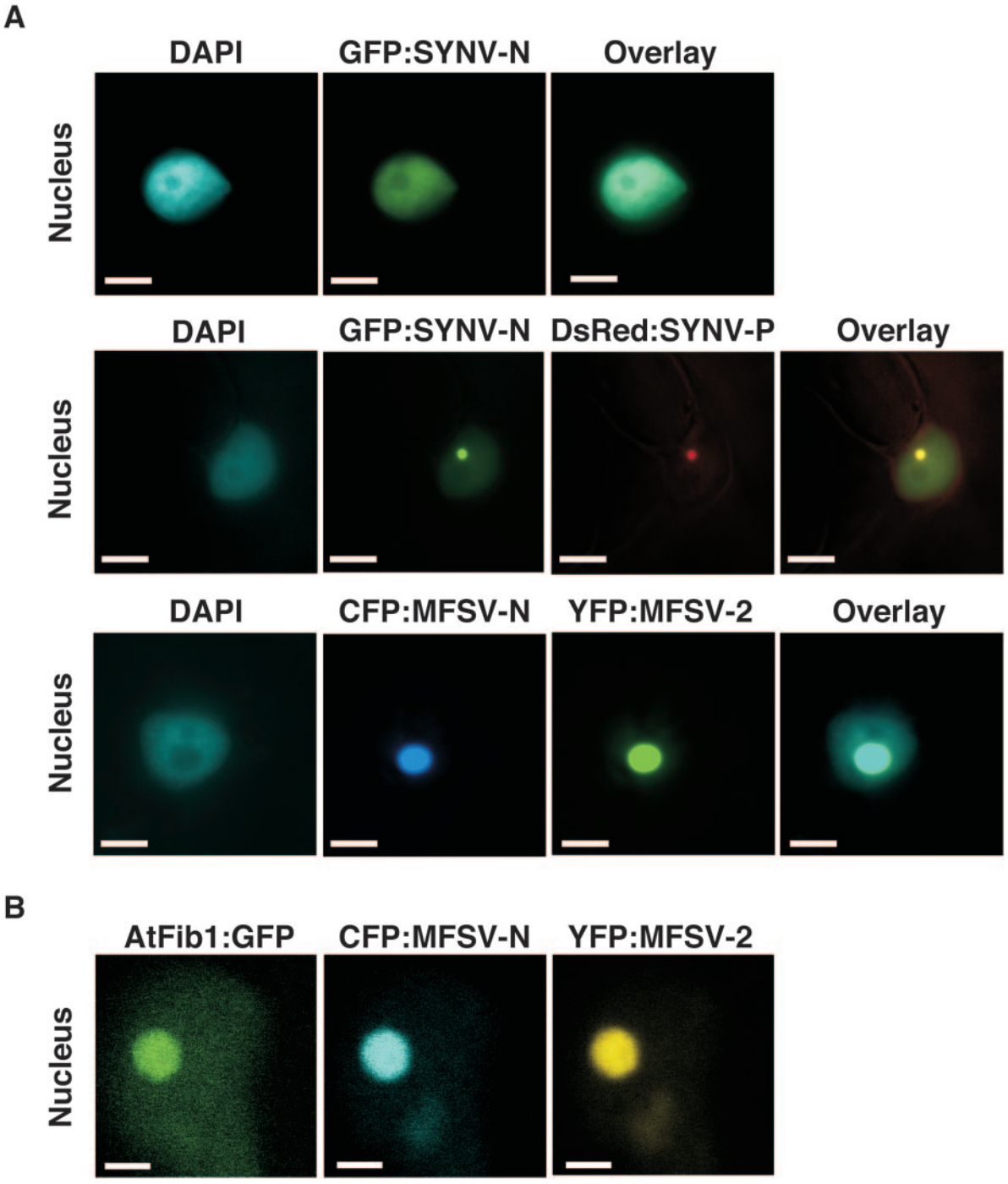

FIG. 8. Subcellular localization of fluorescent-protein fusions of the MFSV N and ORF2 proteins and the SYNV N and P proteins. The DNA selective dye DAPI was used to determine the positions of nuclei in plant cells. (A) Epifluorescence micrographs of GFP-SYNV N infiltrated by itself targeting the nucleus (top row); coinfiltrated GFP-SYNV N and DsRed-SYNV P targeting the subnuclear locale (middle row) (see also Goodin et al. [13]); and coinfiltrated CFP-MFSV N and YFP-MFSV 2 targeting the nucleolus (bottom row). (B) Confocal micrographs of the colocalization of AtFib1-GFP, CFP-MFSV N, and YFP-MFSV 2 in the nucleolus of a plant cell. Single-plane optical sections (0.3 mm thick) for each channel were taken through the largest area of fluorescence within the nucleolus. Bars = 5 μm.

the size of the ORF5 protein are most comparable to the M protein of SYNV (33) and (ii) the ORF5 protein of MFSV targeted the nucleus when expressed alone, similar to the SYNV M protein (13). M protein sequences are not conserved among plant rhabdoviruses, whereas they are conserved among animal- or fish-infecting rhabdoviruses. The M proteins are likely prone to considerable adaptive evolution because these proteins play important roles in the suppression of host transcription (1, 24) and determine budding sites (16, 23).

The MFSV N-P protein complex appears to target a differ-

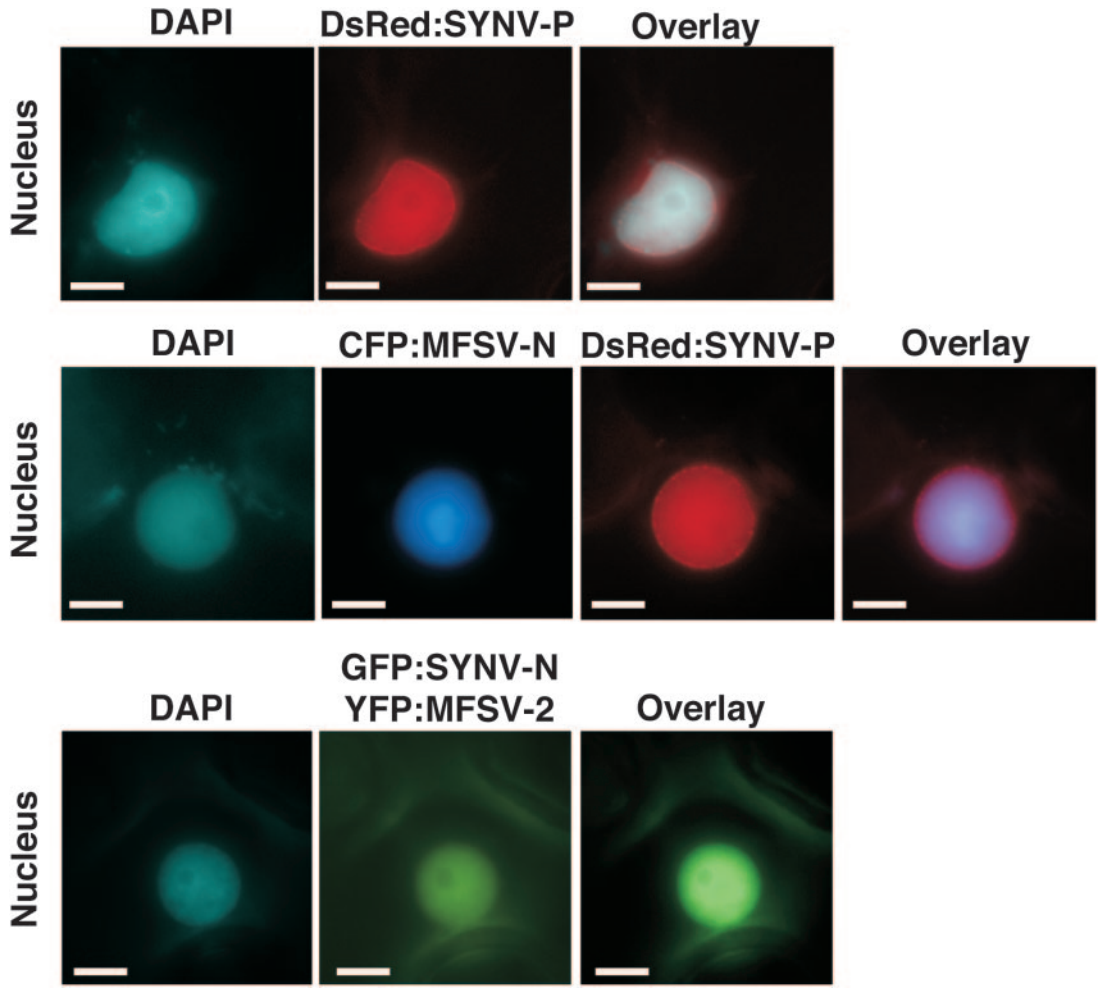

FIG. 9. Epifluorescence micrographs of infiltrated DsRed-SYNV P alone (top row), coinfiltrated CFP-MFSV N and DsRed-SYNV P (middle row), and coinfiltrated GFP-SYNV N and YFP-MFSV 2 (bottom row). The DNA selective dye DAPI was used to determine the positions of nuclei in plant cells. The fluorescences of GFP-SYNV N and YFP-MFSV 2 could not be distinguished by epifluorescence microscopy. Bars = 5 μm.

ent subnuclear locale than the SYNV N-P protein complex. This suggests that there may be differences in the infection mechanisms for the two viruses. However, *N. benthamiana* is a host of SYNV, whereas we have not been able to infect *N. benthamiana* with MFSV by rub inoculation or insect transmission so far (J. C. Todd, S. A. Hogenhout, and M. G. Redinbaugh, unpublished results). More work is needed to determine whether the differential targeting is associated with the abilities of the two viruses to replicate in *N. benthamiana*.

The hypothesis that the infection mechanisms of MFSV and SYNV in plant cells are different is supported by the observation that the subcellular distributions of ORF3 and ORF4 proteins of MFSV were different from the subcellular distribution of the SYNV sc4 protein. The SYNV sc4 protein is a membrane-associated protein, although it does not have a transmembrane domain or an NLS (36). The SYNV sc4 protein has been predicted to be a member of the 30K superfamily of plant virus movement proteins, related to the 30-kDa *Tobacco mosaic virus* (TMV) movement protein (31). All of the sequenced plant rhabdovirus genomes encode a protein of unknown function similar in mass to the 36.7-kDa sc4 protein between the *P* and *M* genes, except for NCMV, which has four small proteins with unknown functions. This unique protein includes the MFSV ORF4 protein, the RYSV 3 protein (4), and the LNYV 4b protein (GenBank accession no. AF209034). Although one is tempted to speculate that, based on similar genome locations and sizes, these additional genes have similar functions, our results show that this may not be the case, because the SYNV sc4 protein is cytosolic (13) while the MFSV ORF4 protein is nuclear.

The interaction of the N and P proteins is specific for MFSV and SYNV; that is, coexpression of the MFSV N protein did not redirect the SYNV P protein to the nucleus, and coexpression of the SYNV N protein did not redirect the MFSV P protein to the nucleus. This is not surprising, given the lack of conservation among plant rhabdovirus P proteins. The P protein acts as a transcription factor and aids in N protein encapsidation of RNA for rhabdoviruses (14). It remains to be investigated whether the interactions between N and P proteins are specific for other rhabdoviruses as well.

The organization of the MFSV genome is distinct from those of other rhabdoviruses described so far because MFSV

TABLE 2. Genome organization of plant rhabdoviruses

Virus	Genome organization	Vector[a]	Host[a]
Nucleorhabdovirus			
MFSV	3′ *N P 3 4 M G L* 5′	L	M
SYNV	3′ *N P sc4 M G L* 5′	A	D
RYSV	3′ *N P 3 M G 6 L* 5′	L	M
Cytorhabdovirus			
LNYV	3′ *N P 4b M G L* 5′	A	D
NCMV	3′ *N P 3 4 5 6 M G L* 5′	P	M

[a] A, aphid; L, leafhopper; P, planthopper; D, dicot; M, monocot.

has two additional genes between the *P* and *M* genes compared to other nucleorhabdoviruses (Table 2). However, the cytorhabdovirus NCMV has four genes between the *P* and *M* genes (39), and the nucleorhabdovirus RYSV has two additional genes, with one located between the *P* and *M* genes and one between the *G* and *L* genes (29) (Table 2). Thus, the locations and numbers of genes, in addition to the basic gene order (3′-*N-P-M-G-L*-5′) (40), vary extensively among insect-transmitted plant rhabdoviruses. All seven ORFs of MFSV were transcribed during the infection of maize, and gene junctions flanked all ORFs. Gene junctions are conserved among plant and animal rhabdoviruses and are important for transcription termination and reinitiation of the rhabdovirus polymerase complex (35).

The MFSV gene junctions suggest that the MFSV genes use UUG as a consensus transcription start site. The RLM-RACE data for the MFSV *G* and *L* genes confirmed this transcription start site. However, a nonviral nucleotide was present at the 5′ ends of MFSV mRNAs. Heterogeneous nucleotides were found at the 5′ ends of viral mRNAs for RYSV and LNYV (29, 42) and were thought to be derived from host cellular RNAs (25). The 3-nucleotide transcription start sites of animal rhabdoviruses and nucleorhabdoviruses are identical, but those of cytorhabdoviruses are clearly different (CUU/A rather than UUG). It is not known whether there is a biological significance in transcription initiation associated with the sequence difference in cytorhabdoviruses.

With the accumulation of completed genome sequences of rhabdoviruses, it is now becoming clear that plant rhabdoviruses are diverse. In this study, we showed for the first time that rhabdoviruses are diverse not only in genome sequence, but also in the subcellular localization of proteins, and hence in the interaction with host factors. It is therefore not surprising that rhabdovirus proteins specifically interact with each other and not with orthologous proteins of another rhabdovirus, as shown here for the N and P proteins of MFSV and SYNV. This information will help to determine factors essential to the host and vector specificities of rhabdoviruses.

ACKNOWLEDGMENTS

The project was supported by the National Research Institute of the USDA Cooperative State Research, Education and Extension Service, grant 2002-35302-12653, and the OARDC research enhancement and competitive grants program.

We thank T. Meulia from the Molecular and Cellular Imaging Center of the OARDC for providing us with a pZeroAmp vector; T. L. German and P. Flanary from the Department of Entomology, University of Wisconsin, for confirming our 3′ and 5′ RACE MFSV sequence results; J. von der Heiden from Leica Microsystems for his excellent technical assistance with acquisition of the confocal micrographs; and R. G. Dietzgen from the Department of Primary Industries and Fisheries, Queensland Government, Australia, for critical reading of the manuscript.

REFERENCES

1. **Ahmed, M., M. O. McKenzie, S. Puckett, M. Hojnacki, L. Poliquin, and D. S. Lyles.** 2003. Ability of the matrix protein of vesicular stomatitis virus to suppress beta interferon gene expression is genetically correlated with the inhibition of host RNA and protein synthesis. J. Virol. **77:**4646–4657.
2. **Barneche, F., F. Steinmetz, and M. Echeverria.** 2000. Fibrillarin genes encode both a conserved nucleolar protein and a novel small nucleolar RNA involved in ribosomal RNA methylation in *Arabidopsis thaliana*. J. Biol. Chem. **275:**27212–27220.
3. **Bendtsen, J. D., H. Nielsen, G. von Heijne, and S. Brunak.** 2004. Improved prediction of signal peptides: SignalP 3.0. J. Mol. Biol. **340:**783–795.
4. **Chen, X. Y., Z. L. Luo, and R. X. Fang.** 1998. Structure analysis of the rice yellow stunt rhabdovirus gene 3. Chinese Sci. Bull. **43:**745–748.
5. **Choi, T. J., S. Kuwata, E. V. Koonin, L. A. Heaton, and A. O. Jackson.** 1992. Structure of the L (polymerase) protein gene of sonchus yellow net virus. Virology **189:**31–39.
6. **Choi, T. J., J. D. Wagner, and A. O. Jackson.** 1994. Sequence analysis of the trailer region of sonchus yellow net virus genomic RNA. Virology **202:**33–40.
7. **Cokol, M., R. Nair, and B. Rost.** 2000. Finding nuclear localization signals. EMBO Rep. **1:**411–415.
8. **Falquet, L., M. Pagni, P. Bucher, N. Hulo, C. J. Sigrist, K. Hofmann, and A. Bairoch.** 2002. The PROSITE database, its status in 2002. Nucleic Acids Res. **30:**235–238.
9. **Fang, R. X., Q. Wang, B. Y. Xu, Z. Pang, H. T. Zhu, K. Q. Mang, D. M. Gao, W. S. Qin, and N. H. Chua.** 1994. Structure of the nucleocapsid protein gene of rice yellow stunt rhabdovirus. Virology **204:**367–375.
10. **Feinberg, A. P., and B. Volgelstein.** 1983. A technique for radiolabeling DNA restriction endonuclease fragments to high specific activity. Anal. Biochem. **132:**6–13.
11. **Goldberg, K. B., B. Modrell, B. I. Hillman, L. A. Heaton, T. J. Choi, and A. O. Jackson.** 1991. Structure of the glycoprotein gene of sonchus yellow net virus, a plant rhabdovirus. Virology **185:**32–38.
12. **Goodin, M. M., J. Austin, R. Tobias, M. Fujita, C. Morales, and A. O. Jackson.** 2001. Interactions and nuclear import of the N and P proteins of sonchus yellow net virus, a plant nucleorhabdovirus. J. Virol. **75:**9393–9406.
13. **Goodin, M. M., R. G. Dietzgen, D. Schichnes, S. Ruzin, and A. O. Jackson.** 2002. pGD vectors: versatile tools for the expression of green and red fluorescent protein fusions in agroinfiltrated plant leaves. Plant J. **31:**375–383.
14. **Gupta, A. K., D. Shaji, and A. K. Banerjee.** 2003. Identification of a novel tripartite complex involved in replication of vesicular stomatitis virus genome RNA. J. Virol. **77:**732–738.
15. **Hanson, M. R., and R. H. Kohler.** 2001. GFP imaging: methodology and application to investigate cellular compartmentation in plants. J. Exp. Bot. **52:**529–539.
16. **Harty, R. N., J. Paragas, M. Sudol, and P. Palese.** 1999. A proline-rich motif within the matrix protein of vesicular stomatitis virus and rabies virus interacts with WW domains of cellular proteins: implications for viral budding. J. Virol. **73:**2921–2929.
17. **Heaton, L. A., D. Zuidema, and A. O. Jackson.** 1987. Structure of the M2 protein gene of sonchus yellow net virus. Virology **161:**234–241.
18. **Heaton, L. A., B. I. Hillman, B. G. Hunter, D. Zuidema, and A. O. Jackson.** 1989. Physical map of the genome of sonchus yellow net virus, a plant rhabdovirus with six genes and conserved gene junction sequences. Proc. Natl. Acad. Sci. USA **86:**8665–8668.
19. **Hillman, B. I., L. A. Heaton, B. G. Hunter, B. Modrell, and A. O. Jackson.** 1990. Structure of the gene encoding the M1 protein of sonchus yellow net virus. Virology **179:**201–207.
20. **Hogenhout, S. A., M. G. Redinbaugh, and E.-D. Ammar.** 2003. Plant and animal rhabdovirus host range: a bug's view. Trends Microbiol. **11:**264–271.
21. **Huang, Y., H. Zhao, Z. Luo, X. Chen, and R. X. Fang.** 2003. Novel structure of the genome of Rice yellow stunt virus: identification of the gene 6-encoded virion protein. J. Gen. Virol. **84:**2259–2264.
22. **Jackson, A. O., M. Goodin, I. Moreno, J. Jackson, and D. M. Lawrence.** 1999. Plant rhabdoviruses, p. 1531–1541. *In* A. Granoff and R. G. Webster (ed.), Encyclopedia of virology. Academic Press, San Diego, Calif.
23. **Jayakar, H. R., and M. A. Whitt.** 2002. Identification of two additional translation products from the matrix (M) gene that contribute to vesicular stomatitis virus cytopathology. J. Virol. **76:**8011–8018.
24. **Kopecky, S. A., and D. S. Lyles.** 2003. Contrasting effects of matrix protein on apoptosis in HeLa and BHK cells infected with vesicular stomatitis virus are due to inhibition of host gene expression. J. Virol. **77:**4658–4669.
25. **Krug, R. M.** 1981. Priming of influenza viral RNA transcription by capped heterologous RNAs. Curr. Top. Microbiol. Immunol. **93:**125–149.
26. **Kurath, G., K. H. Higman, and H. V. Bjorklund.** 1997. Distribution and variation of NV genes in fish rhabdoviruses. J. Gen. Virol. **78:**113–117.

27. **Louie, R.** 1995. Vascular puncture of maize kernels for the mechanical transmission of maize white line mosaic virus and other viruses of maize. Phytopathology **85:**139–143.
28. **Luo, Z., X. Chen, D. Gao, and R. Fang.** 1998. The gene 4 of rice yellow stunt rhabdovirus encodes the matrix protein. Virus Genes **16:**277–280.
29. **Luo, Z. L., and R. X. Fang.** 1998. Structure analysis of the rice yellow stunt rhabdovirus glycoprotein gene and its mRNA. Arch. Virol. **143:**2453–2459.
30. **McWilliam, S. M., K. Kongsuwan, J. A. Cowley, K. A. Byrne, and P. J. Walker.** 1997. Genome organization and transcription strategy in the complex G_{NS}-L intergenic region of bovine ephemeral fever rhabdovirus. J. Gen. Virol. **78:**1309–1317.
31. **Melcher, U.** 2000. The '30K' superfamily of viral movement proteins. J. Gen. Virol. **81:**257–266.
32. **Redinbaugh, M. G., G. J. Wadsworth, and J. G. Scandalios.** 1988. Characterization of catalase transcripts and their differential expression in maize. Biochem. Biophys. Acta **951:**104–116.
33. **Redinbaugh, M. G., and S. A. Hogenhout.** 2005. Plant rhabdoviruses, p. 143–163. *In* Z. Fu and H. Koprowski (ed.), Current topics in microbiology and immunology, vol. 292. The world of rhabdoviruses. Springer-Verlag, New York, N.Y.
34. **Redinbaugh, M. G., D. L. Seifers, T. Meulia, J. J. Abt, R. J. Anderson, W. E. Styer, J. Ackerman, R. Salomon, W. Houghton, R. Creamer, D. T. Gordon, and S. A. Hogenhout.** 2002. Maize fine streak virus, a new leafhopper-transmitted rhabdovirus. Phytopathology **92:**1167–1174.
35. **Rose, J. K., and M. A. Whitt.** 2001. Rhabdoviridae: the virus and their replication, p. 1221–1244. *In* D. M. Knipe and P. M. Howely (ed.), Fields virology. Lippincott Williams & Wilkins, Philadelphia, Pa.
36. **Scholthof, K. B., B. I. Hillman, B. Modrell, L. A. Heaton, and A. O. Jackson.** 1994. Characterization and detection of sc4: a sixth gene encoded by sonchus yellow net virus. Virology **204:**279–288.
37. **Sonnhammer, E. L. L., G. von Heijne, and A. Krogh.** 1998. A hidden Markov model for predicting transmembrane helices in protein sequences, p. 175–182. *In* J. Glasgow, T. Littlejohn, F. Major, R. Lathrop, D. Sankoff, and C. Sensen (ed.), Proceedings of the Sixth International Conference on Intelligent Systems for Molecular Biology. AAAI Press, Menlo Park, Calif.
38. **Stewart, C. N.** 2001. The utility of green fluorescent protein in transgenic plants. Plant Cell Rep. **20:**376–382.
39. **Tanno, F., A. Nakatsu, S. Toriyama, and M. Kojima.** 2000. Complete nucleotide sequence of northern cereal mosaic virus and its genome organization. Arch. Virol. **145:**1373–1384.
40. **Walker, P. J., A. Benmansour, R. Dietzgen, R. X. Fang, A. O. Jackson, G. Kurath, J. C. Leong, S. Nadin-Davies, R. B. Tesh, and N. Tordo.** 2000. Family Rhabdoviridae, p. 563–583. *In* M. H. V. van Regenmortel, C. M. Fauquet, D. H. L. Bishop, E. B. Carstens, M. K. Estes, S. M. Lemon, J. Maniloff, M. A. Mayo, D. J. McGeoch, C. R. Pringle, and R. B. Wickner (ed.), Virus taxonomy: classification and nomenclature of viruses. Seventh report of the International Committee on Taxonomy of Viruses. Academic Press, San Diego, Calif.
41. **Wang, Q., X. Y. Chen, Z. L. Luo, and R. X. Fang.** 1999. Sequence analysis of leader and trailer regions of rice yellow stunt rhabdovirus and characterization of their in vivo transcripts. Sci. China Ser. C **42:**50–56.
42. **Wetzel, T., R. G. Dietzgen, and J. L. Dale.** 1994. Genomic organization of lettuce necrotic yellows rhabdovirus. Virology **200:**401–412.
43. **Zhu, H. T., X. Y. Chen, Z. L. Luo, R. X. Fang, and D. M. Gao.** 1997. Nucleotide sequence of the rice yellow stunt rhabdovirus gene 2. Chinese J. Virol. **13:**369–375.
44. **Zuidema, D., L. A. Heaton, R. Hanau, and A. O. Jackson.** 1986. Detection and sequence of plus-strand leader RNA of sonchus yellow net virus, a plant rhabdovirus. Proc. Natl. Acad. Sci. USA **83:**5019–5023.
45. **Zuidema, D., L. A. Heaton, and A. O. Jackson.** 1987. Structure of the nucleocapsid protein gene of Sonchus yellow net virus. Virology **159:**373–380.